Research Article

Joanna Korzekwa*, Michał Fal, and Aneta Gądek-Moszczak

DOE Application for Analysis of Tribological Properties of the Al_2O_3/IF-WS_2 Surface Layers

https://doi.org/10.1515/eng-2021-0012
Received Mar 02, 2020; accepted Oct 18, 2020

Abstract: The article presents the effect of the processing parameters on tribological properties of aluminum oxide coatings Al_2O_3 doped with fullerene-like tungsten disulfide (IF-WS_2) by design of experiment (DOE). Anodic oxidation of aluminum alloy was carried out in a ternary solution of SAS (sulfuric, adipic and oxalic acids) with IF-WS_2. The thickness, geometric structure of the surface (SGP) and the tribological properties such as friction coefficient of tribological pair: Al_2O_3/IF-WS_2 with polieteroeteroketon filled with graphite, carbon fiber and PTFE (named PEEK/BG) were investigated. The influence of electrolysis time and temperature on the tribological properties of coatings was studied using 2^k factorial design. The stabilization of the friction coefficient indicates generation of steady anti-wear and anti-seizure Al_2O_3/IF-WS_2 oxide coatings. DOE suggest i.e. high positive correlation between oxide thickness and time and temperature of the anodizing process.

Keywords: coating, friction coefficient, texture, surface roughness, DOE

1 Introduction

Tribotesting of friction systems needs a discussion on the proper selection of its conditions and data presentation. The reliability of elements during tribological friction depends largely on the quality and condition of the surface layers involved in the mechanism of friction. In oil-less tribological coupling the choice of type of materials for tribological pair plays an important role. Light weight, quite large corrosion resistance, a simplicity of surface treatment and forming, a total process ability as a secondary raw material are just few benefits of aluminum alloys which are widely used in motorization, aircraft or food industry. Aluminum alloys have high friction coefficient wherefore without appropriate surface treatment it is unsuitable as friction material. To improve poor wear or/and corrosion resistance of aluminum, various methods such as hard anodizing [1–4], sol-gel coating [5, 6], lubricating additives [7, 8], anodic oxidation [9–11] and polymer coating [12, 13], have been applied. The tribological partner in the sliding nodes can be a plastic (for acetabular bearings, guides and seals) with selected properties improved in different directions. The following can be included in the group of thermoplastic materials used in the construction of sliding machine elements: polyether ether ketone (PEEK), polytetrafluoroethylene (PTFE), polyamide (PA), graphite, carbon fiber and PTFE-called PEEK/BG and others [8, 14–17].

It is known that the frictional resistance depends on the load, sliding velocity of frictional nodes and is also influenced by humidity or surface property parameters (such as roughness and topography). The properties of anodized aluminum oxide layer depend on such parameters of technological process as current density, kind of electrolyte, temperature and time of electrolysis. In the literature limited information is available regarding how Al_2O_3/IF-WS_2 coatings build up and how their tribological properties are determined by anodizing technological parameters. Our approach and research concerning Al_2O_3/IF-WS_2 coatings and PEEK/BG plastic may be useful for application in oil-less tribo-pairs e.g. pneumatic cylinders.

Experimental design or design of experiment (DOE) is a systematic approach to understand how process and product parameters affect response variables such as process ability, physical properties, or product performance. DOE is used to determine which factors or variables and their interactions are most important and also those that are insignificant in the analyzed process [18, 19]. Pierlot at al used DOE methodology for thermal spraying

***Corresponding Author: Joanna Korzekwa:** Faculty of Science and Technology, Institute of Materials Engineering, University of Silesia in Katowice, 75 Pułku Piechoty 1a, 41–500 Chorzów, Poland; Email: joanna.korzekwa@us.edu.pl
Michał Fal: Faculty of Science and Technology, Institute of Materials Engineering, University of Silesia in Katowice, 75 Pułku Piechoty 1a, 41–500 Chorzów, Poland; Email: mf543@gazeta.pl
Aneta Gądek-Moszczak: Cracow University of Technology, Faculty of Mechanical Engineering, Al. Jana Pawla II 37, 31-864 Krakow, Poland, EU; Email: aneta.gadek-moszczak@pk.edu.pl

and associated processes of post-spray treatment [20]. Authors [21] studied the advanced statistical refinement of surface layer's discretization in the case of electro-spark deposited Mo coatings. Investigations included an experiment based on the static, determined, multi-factor, and rotatable design with PS/DS-l repetitions. The design of experiments technique at a two-level factorial and a central composite rotatable design was used to analyze and optimize the HVOF spraying process [22].

This paper aims at correlating two anodizing processing parameters – time and temperature, and checking how they affected the formation of the Al_2O_3/IF-WS_2 coating by evaluating response variables, viz., oxide thickness, *Ra* surface roughness parameter and friction coefficient. The 2^k factorial design and multiply regression were used to determine the influence electrolysis time and temperature on the tribological properties of coatings. The independent variables for this investigation were the high (+1) and low (–1) levels of temperature and time of electrolysis and thickness, friction coefficient and surface roughness parameters were the dependent variables.

2 Experimental part

2.1 Methodological bases

The framework structure of this study is illustrated in Figure 1. Macroscopic images of the samples were made with an Omnivision OV12A10 camera (Xiaomi Redmi 5 Plus) and an Olympus BX60M optical microscope with a Motic camera. The thickness of the layers was measured with a Dualscope MP40 by Fischer, using the eddy current method. 10 measurements were performed along the length of the sample and the average value was calculated. SGP measurements of oxide layers were made by at Taylor Hobson Talysurf 3D pin profilometer with the accuracy of 2%. The results of the parameters were developed by using at TalyMap Universal 3D software. The stereometric analysis was performed on an area of 2 mm × 2 mm. Tribological measurements were performed on a T17 tester (ITeE, Radom), using a pin-on-plate arrangement with reciprocating motion. The conditions under which tribological measurements were carried out are: room temperature, humidity of 35±5%, pressure of 0.5 MPa and sliding speed of 0.2 m/s under dry friction conditions.

The tribological test was conducted over a sliding distance of 15 km which allows for the completion of the running-in stage and for the observation of the stabilization of the friction coefficient course. A commercial PEEK/BG plastic pin of a diameter of 9 mm was used as a counter-body. The average value of friction coefficient, used in design of experiment, was calculated at the point at which the friction coefficient reached the rectilinear range. After each friction process, wear of the PEEK/BG plastic was quantified gravimetrically using a WPA-60G (Radwag) analytical balance to an accuracy of 0.1 mg.

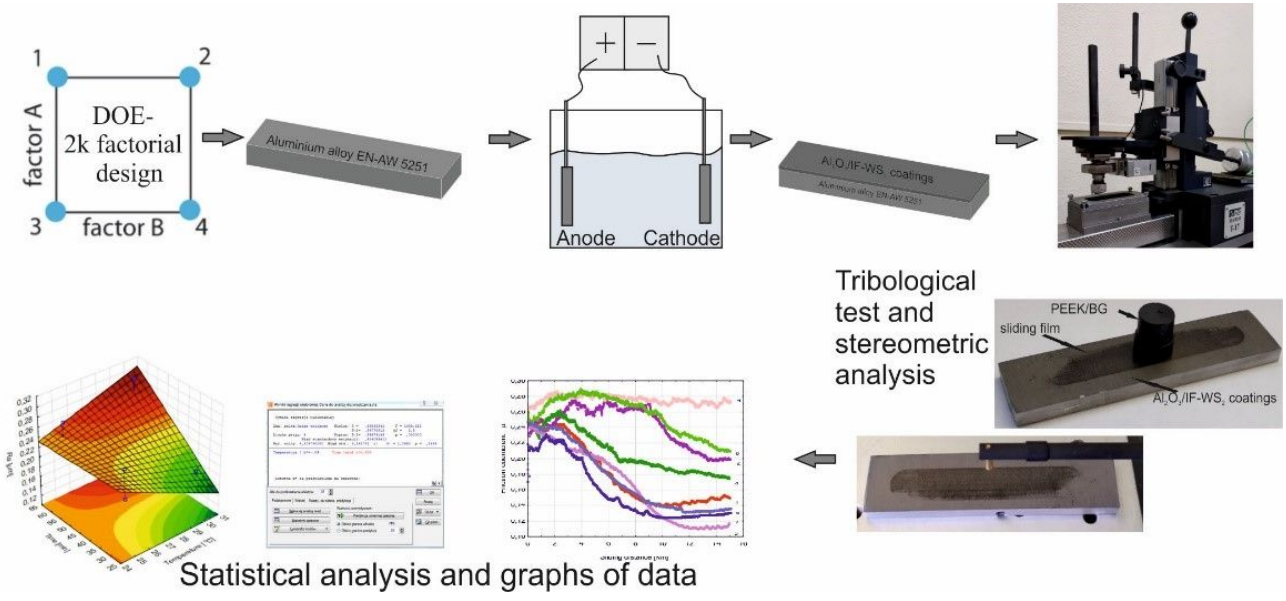

Figure 1: Framework structure of this study

2.2 Sample preparation

EN-AW-5251 aluminum alloy was the starting material for the process. Samples were etched sequentially with a 5% KOH solution for 45 minutes, and 10% HNO_3 solution for 10 minutes, at room temperature. After each step of etching, the sample was placed in distilled water to remove residual acid. The electro-oxidation of the aluminum alloy was carried out in a SAS ternary solution (18% sulfuric (33 ml/l), adipic (67 g/l) and oxalic acids (30 g/l)) with admixture of 15 g of the commercially available IF-WS_2 nanoparticles (NanoMaterials Ltd) per 1 liter of electrolyte. The hard anodizing process was performed at 3 A/dm^2 current density. In order to ensure homogeneity of the suspension and to prevent settling of the IF-WS_2 nanopowder, mechanical stirring was applied during the electrolysis process.

2.3 Experimental design

The 2^k factorial design with one repetition was implemented for analyzing the influence of the technological process parameters on thickness, friction coefficient and surface roughness parameter of Al_2O_3/IF-WS_2 coatings. A two-level factorial design of experiments was applied. It was decided that the best independent variables for this investigation were the high (+1) and low (–1) levels of temperature and time of electrolysis and the thickness, friction coefficient and surface roughness parameter the dependent variables. Benchmark analysis of all dependent variables against a factorial design and a two-factor model with second-order interaction was carried out. A Pareto chart was chosen because it is one of the most rapid ways to determine which of the different factors has the greatest influence on the process. It is usually used to determine the magnitude and the importance of the effects. For the interpretation of the statistical significance of factors on the process in statistical software the p-value is commonly used. In Pareto chart those bars that cross the reference line (in present article p-value = 0, 05) are statistically significant at the 0.05 level. The statistical analysis used in this article included also the two-factor equation with second-order interaction will estimate a linear equation of the following form:

$$z = \mu + \alpha_i + \beta_j + \gamma_{ij} \quad (1)$$

where:
Z – dependent variable (at the present article namely as thickness, friction coefficient, surface roughness Ra),
μ – average process response,
α_i – the effect of the first factor at the i level,
β_j – the effect of the second factor at the j level,
γ_{ij} – second-order interaction effect at the i-th level of the first factor and at the j-th level of the second factor.

It was decided that a 3D scatter chart and a Pareto chart of standardized effects and the normal probability plot of residual for dependent variables were the best graphs for this study. Pearson's correlation coefficients were used to quantify the degree of correlation between dependent and independent variables. Pearson r correlation is the most widely used correlation statistic to measure the degree of the relationship between linearly related variables. The statistical significance of the correlations were assessed using an α-value of 0.05. The accepted values of the correlation coefficient for the "goodness" of fit are given in Table 1 [23]. Statistica 13.1 (TIBCO Software Inc) was the software program used to analyze the data. The coded values assigned to each of the independent variables in our 2^k design are presented in Table 2.

Table 1: Rule of a thumb for interpreting the size of a correlation coefficient

Size of correlation	Independent variables
0.90 to 1.00 (–0.90 to –1.00)	Very high positive (negative) correlation
0.70 to 0.90 (–0.70 to –0.90)	High positive (negative) correlation
0.50 to 0.70 (–0.50 to –0.90)	Moderate positive (negative) correlation
0.30 to 0.50 (–0.30 to –0.50)	Low positive (negative) correlation
0.00 to 0.30 (0.00 to –0.30)	Negligible correlation

3 Results and discussion

The influence of technology parameters on oxide thickness

These tests showed that the oxide thickness takes values from 24.61 μm for sample No 7 to 53.81 μm for sample No 5 (Table 2). The scatter chart of oxide thickness over time and temperature of anodizing process are depicted in Figure 2a. The marginal means plot for the oxide thickness vs. time is shown in Figure 2b. The confidence intervals are set for 95%. As expected our experiment demonstrates strong dependency of oxide thickness on time. The anodizing of aluminum alloy for 30 minutes allow for obtaining the oxide

Table 2: Factor settings for 2^k factorial design

	Independent variables			Dependent variables		
Factor / sample name	**Temperature [°C]**	**Time [min]**	**Oxide thickness [µm]**	***Ra* parameter before tribological test [µm]**	**Friction coefficient [μ]**	***Ra* parameter after tribological test [µm]**
1	25 (−1)	30 (−1)	26.19±0.31	0.20±0.04	0.144±0.001	0.13±0.03
2	25 (−1)	60 (+1)	52.93±0.46	0.27±0.06	0.199±0.001	0.15±0.03
3	30 (+1)	60 (+1)	53.66±0.41	0.25±0.07	0.180±0.002	0.16±0.05
4	25 (−1)	30 (−1)	27.45±0.33	0.26±0.05	0.273±0.003	0.22±0.07
5	25 (−1)	60 (+1)	53.81±0.39	0.21±0.05	0.112±0.002	0.12±0.02
6	30 (+1)	60 (+1)	52.42±0.16	0.30±0.06	0.211±0.001	0.17±0.05
7	30 (+1)	30 (−1)	24.61±0.43	0.19±0.06	0.126±0.002	0.16±0.03
8	30 (+1)	30 (−1)	25.64±0.39	0.16±0.03	0.134±0.002	0.13±0.03

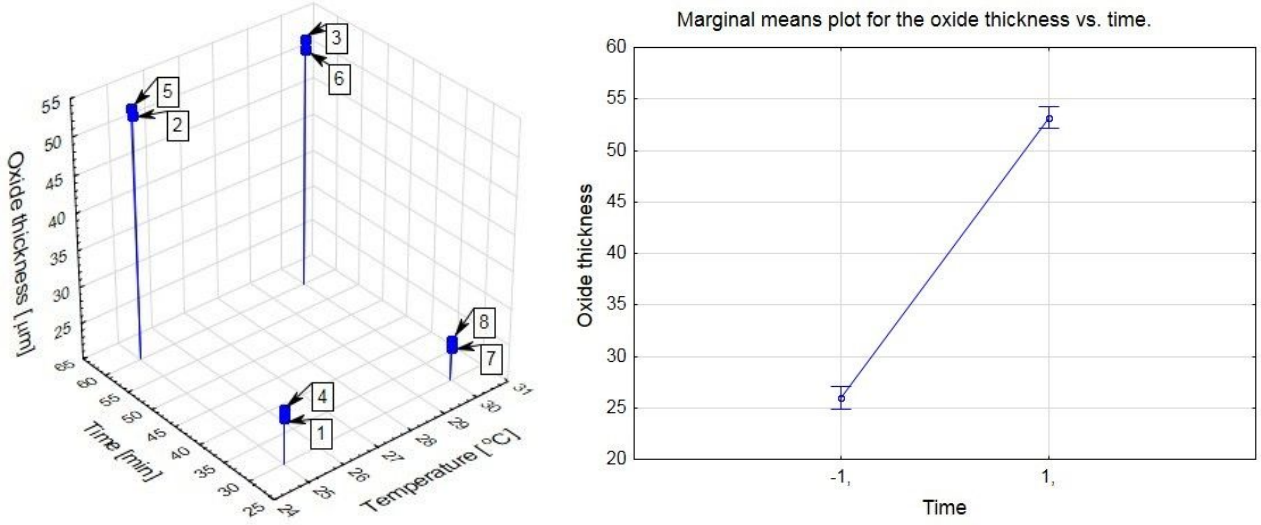

Figure 2: (a) The scatter chart of oxide thickness over time and temperature of anodizing process; (b) Marginal means plot for the oxide thickness vs. time. The confidence intervals are set for 95%

with thickness above 20 µm, which is a satisfactory value for a tribological test.

The Pareto chart of standardized effect for oxide thickness variable for a two-factor model with interaction is shown in Figure 3a. On the Pareto chart in Figure 3a bar that crosses the reference line (time of anodizing process) is statistically significant at the 0.05 level. The multiple correlation coefficient r was 0.99; therefore according to Table 1 the independent variables exhibited very high positive correlation. The two-factor equation with second-order interaction is described by the following equation:

$$z\,(oxide\ thickness) = 39,59 + 27,23\ time - 1,01\ temperature + 0,68 \quad (2)$$

where: time, temperature – level setting in coded values (−1,+1)

In Figure 3b the graph of normal probability plot of residual for oxide thickness variable for a two-factor model with interaction are presented. One can observe deviate from the straight line (S-shaped around the line) which means that the residuals are not normally distributed. In order to shorten the caudal distribution area, a one-factor model was used, taking into account a significant factor, i.e. time. The Pareto chart of standardized effect and normal probability plot of residual for oxide thickness variable for oxide thickness variable for a for a linear univariate model are shown in Figure 3a and 3b respectively.

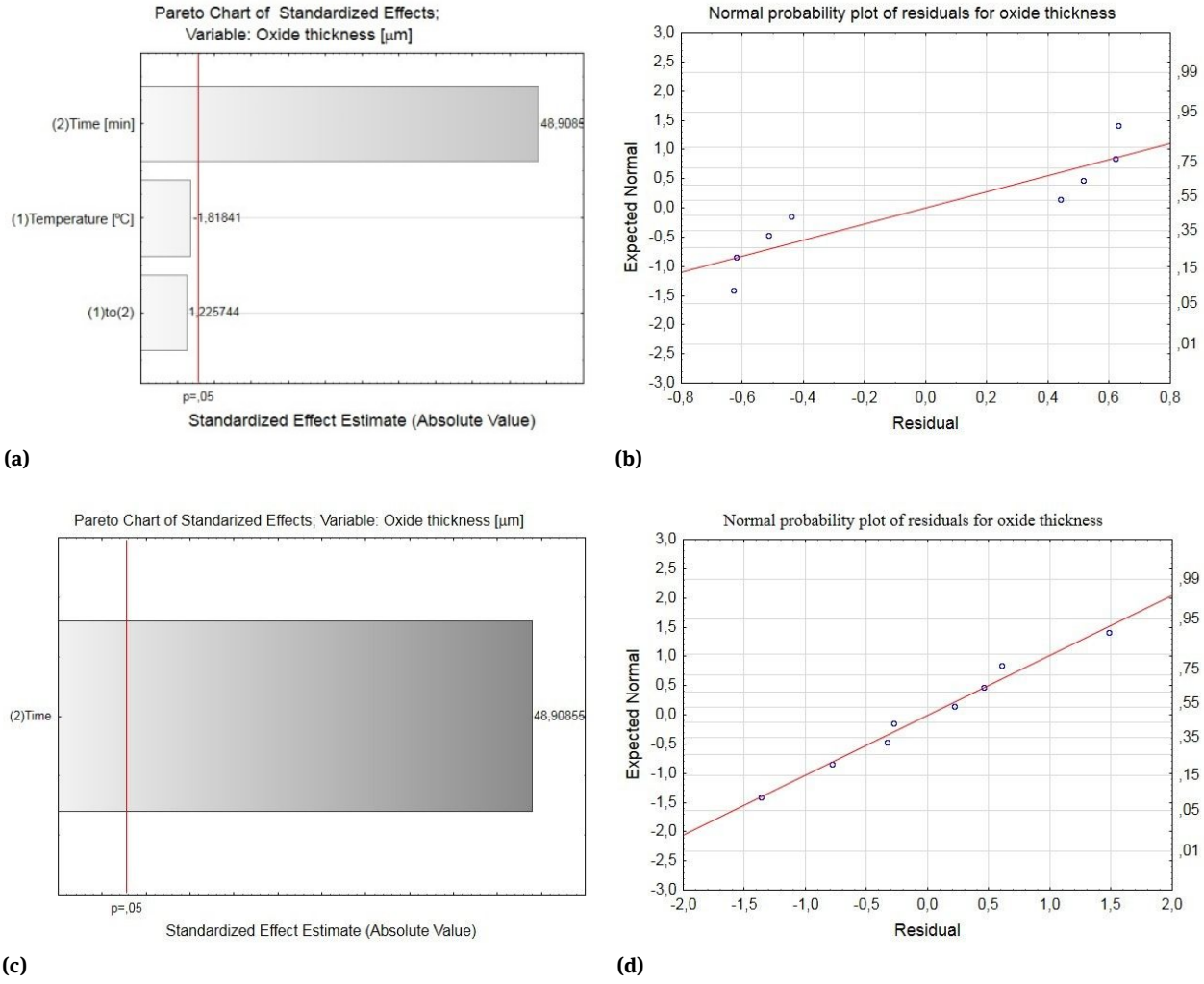

Figure 3: Two-factor model with interaction (a) The Pareto chart of standardized effects for oxide thickness, (b) the normal probability plot of residual for oxide thickness variable; Linear univariate model (c) The Pareto chart of standardized effects for oxide thickness, (d) the normal probability plot of residual for oxide thickness variable

The influence of technology parameters on surface roughness

The surface roughness is an important parameter to take into account when the aluminum oxide layers of high quality must be obtained. The surface pretreatment must be carefully selected to clean the natural surface oxides and to reduce the number of intermetallic compounds present on the surface. Moreover, to reduce the surface roughness, additional steps must be included, such as chemical or mechanical polishing and electro polishing [24]. Further examinations showed that the surface roughness value after anodizing process and before tribological test were in the range of 0.16 for sample No 8 to 0.30 µm for sample No 6, while after the tribological test were in the range of 0.12 for sample No 5 to 0.22 µm for sample No 4 (Table 2). The scatter charts of *Ra* surface roughness parameter before and after the tribological test over time and temperature of anodizing process are depicted in Figure 4a and 4b respectively. It could be concluded that for each samples the surface roughness decrease after the tribological test.

The Pareto charts of standardized effect for *Ra* surface roughness variable before and after the tribological test are shown in Figure 5a and b respectively. On the Pareto charts in Figure 5a and 5b the bars did not cross the reference line. From the statistical point of view it means that the variables are statistically insignificant at the 0.05 level. According to [24] and the obtained statistical information these results thus need to be interpreted with caution. Further data collection is required to determine exactly which variables affect surface roughness in the anodizing pro-

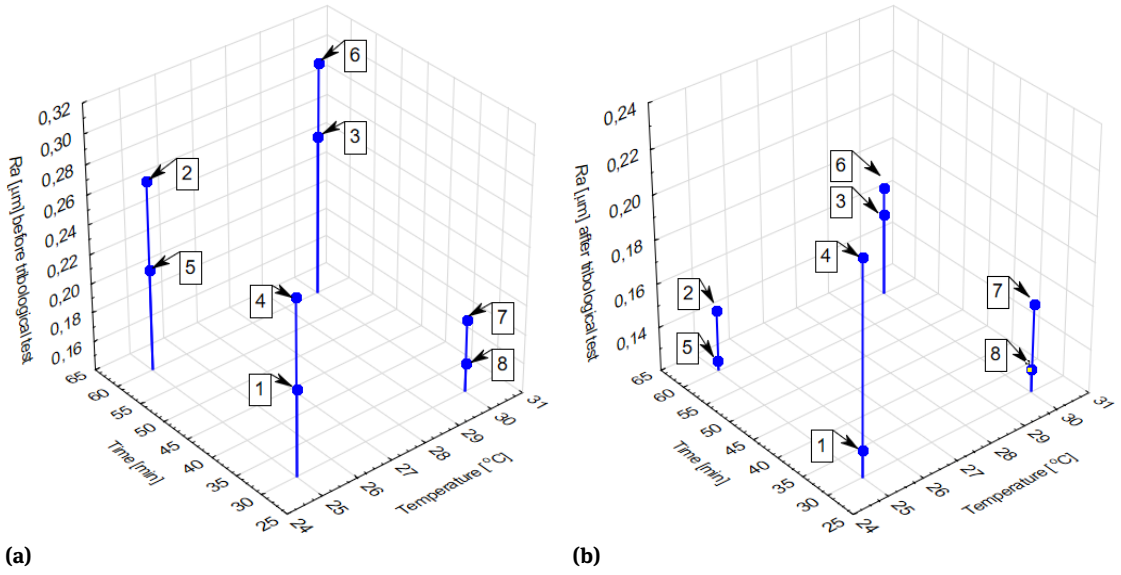

Figure 4: The scatter charts of *Ra* surface roughness over time and temperature of anodizing process a) before b) after tribological test

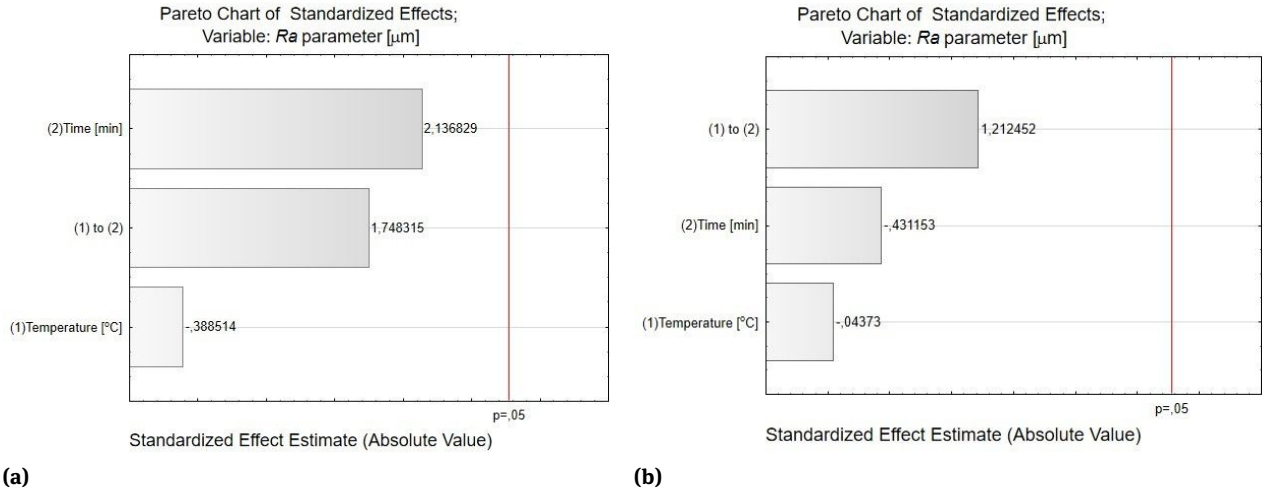

Figure 5: The Pareto chart of standardized effects for *Ra* surface roughness (a) before the tribological test, (b) after the tribological test

cess of Al_2O_3/IF-WS_2 surface layer. Despite the fact mentioned above, the multiple correlation coefficients r was 0.63 and 0.18 for surface roughness parameters before and after the tribological test respectively. Therefore according to Table 1, the independent variables exhibited moderate positive correlation and negligible correlation respectively. The two-factor equation with second-order interaction for *Ra* surface roughness parameters before tribological test is described in the following equation:

$$z\,(Ra\ parameter\ before\ tribological\ test) = 0,23 + 0,05\ time - 0,01\ temperature + 0,04 \quad (3)$$

where: time, temperature – level setting in coded values (–1,+1)

While for *Ra* surface roughness parameters after tribological test described equation:

$$z\,(Ra\ parameter\ after\ tribological\ test) = 0,15 - 0,01\ time + 0,03 \quad (4)$$

where: time, temperature - level setting in coded values (–1,+1)

In Figure 6 the graphs of normal probability plot of residual for *Ra* surface roughness (a) before the tribological test, (b) after the tribological test variables were presented. For *Ra* surface roughness before tribological test

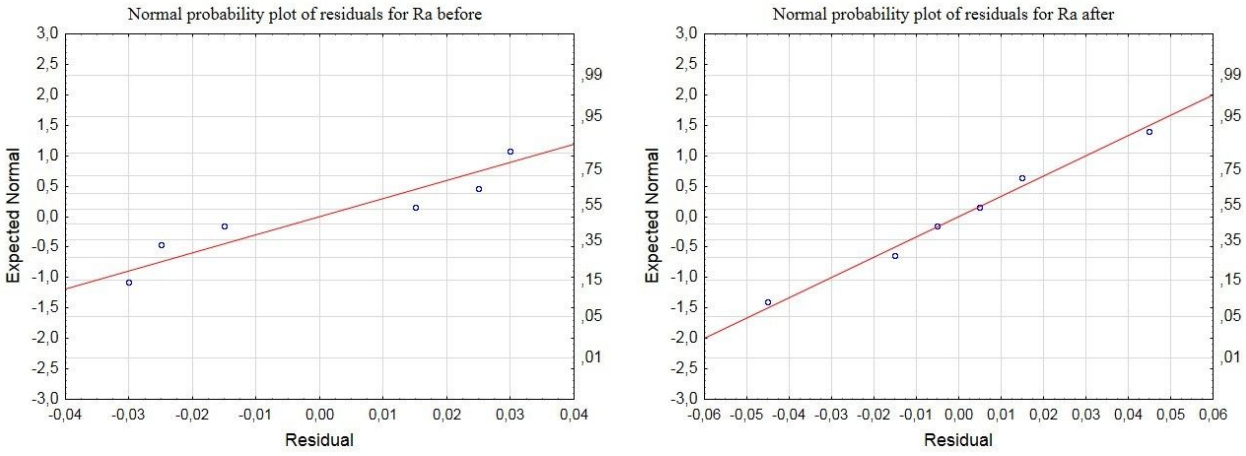

(a) (b)

Figure 6: Graphs of the normal probability plot of residual for *Ra* surface roughness (a) before the tribological test, (b) after the tribological test

(Figure 6a) the deviate from the straight line (S-shaped around the line) is observed which means that the residuals are not normally distributed while for *Ra* surface roughness after tribological test (Figure 6b) the data is from a normally distributed population.

The influence of technology parameters on friction coefficient

No significant influence was identified in this study among time, temperature and friction coefficient. However, correlation between friction coefficient and technological parameters is worth mentioning because most of the study pays attention generally to dependency of temperature on morphological or mechanical properties of layers [25, 26].

Friction coefficient μ between Al_2O_3/IF-WS_2 surface layer and PEEK/BG pin reached the value from $\mu = 0.11$ for sample No 5 to $\mu = 27$ for sample No 4. The scatter chart of friction coefficient over time and temperature of anodizing process are depicted in Figure 7a, while the graphs which show dependence of friction coefficient versus sliding distance is shown in Figure 5b. Samples No 1 and No

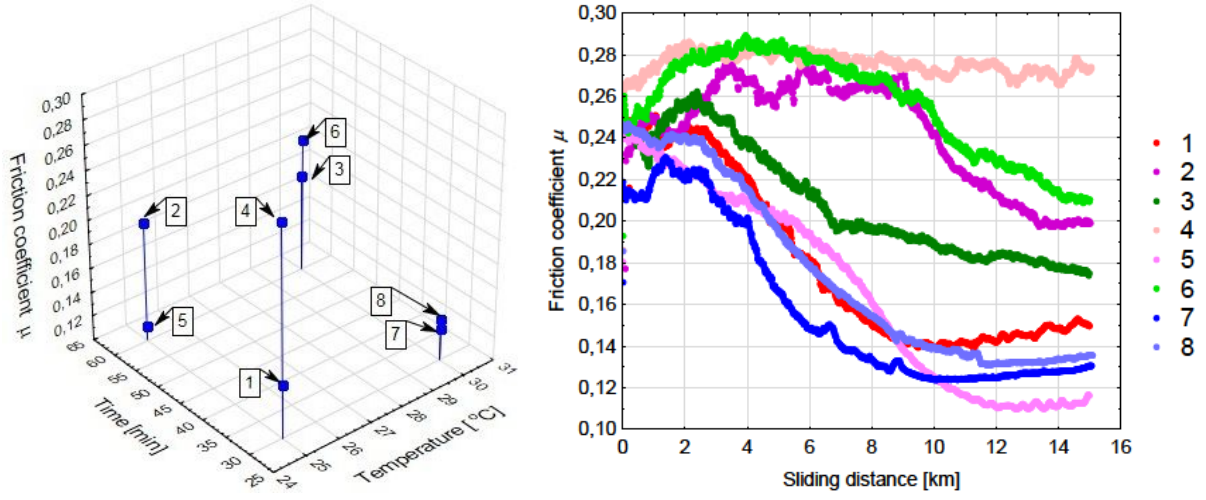

(a) (b)

Figure 7: a) The scatter chart of friction coefficient μ over time and temperature of anodizing process, b) diagram of friction coefficient versus sliding distance

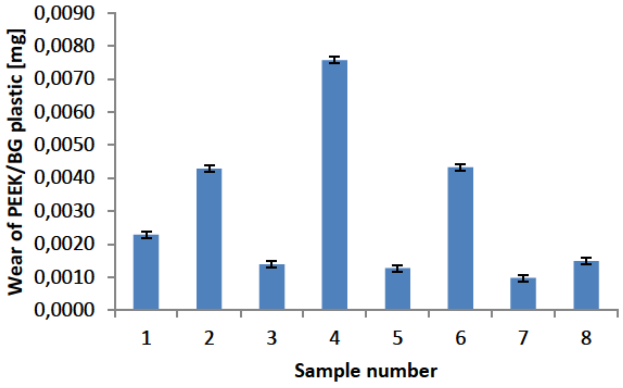

Figure 8: A bar graph of mass loss of PEEK/BG plastic

Table 3: The mass loss of PEEK/BG plastic

Sample number	Wear of PEEK/BG plastic [mg] ±0.0001
1	0.0023
2	0.0043
3	0.0014
4	0.0076
5	0.0013
6	0.0043
7	0.0010
8	0.0015

4 were obtained in the same technological parameters but as is shown in Figure 7b exhibited different kind of course of friction coefficient. For sample No 4 one can observe a rather stable value of friction coefficient from the second km of the sliding distance. For other cases the tribological tests revealed that running-in of the friction couple occurred. The distance where the sliding couples reached stabilized friction coefficient (the rectilinear part) was different for each couples. Contrary to the expectations we did not find significant similarities for samples obtained in the same technological condition expect samples No 7 and 8. Broadly speaking, we found that after different time of sliding, the friction coefficients remained stable. We believe that our findings compare well with the opinion that the most favorable operating conditions are present in sliding pairs in which the friction coefficient increases in the initial stage of start-up, and then decreases significantly and stabilizes itself at a constant level [27].

In Figure 8, a bar graph of mass loss of PEEK/BG polymer was presented. The higher values of mass loss were noticed for polymers during tribological friction with samples 2, 4 and 6 which were also characterized by the higher values of surface roughness (Table 2) and also the higher values of friction coefficient (Figure 7). Sample 4 did not show the course of the friction coefficient characterized by the running-in stage (Figure 7b), for samples 2 and 6 the run-in time was long and a stable friction coefficient was achieved until around 14 km of the friction path. The lower values of surface roughness were observed for samples 1,5,7,8 (Table 2). For those samples, also the friction coefficient is low and at relatively stable chart of the friction coefficient was observed around 10 km of the friction path. The mass loss of PEEK/BG polymers during tribological friction with samples 5, 7 and 8 (Figure 8) were also low.

The Pareto chart of standardized effect for friction coefficient μ variable is shown in Figure 9a. On the Pareto chart in Figure 9a, the bars did not cross the reference line. From the statistical point of view it means that the variables are statistically insignificant at the 0.05 level. The multiple correlation coefficient r was 0.33; therefore, according to Table 1 the independent variables exhibited low positive correlation. The normalized form of the regression for oxide thickness is described by the following equation:

$$z\,(Friction\ coefficient\ \mu) = 0,17 + 0,006\ time - 0,019\ temperature + 0,059 \quad (5)$$

where: time, temperature – level setting in coded values (−1,+1)

In Figure 9b the graphs of the normal probability plot of residual for friction coefficient μ was presented. The data is from a normally distributed population.

The performance concerning high friction coefficient for sample No 4 was slightly disappointing. This was probably a result of the higher value of surface roughness parameter *Ra* and also lower value of the thickness coating. This suggestion is in good agreement with Yerokhin *et al.* [28] which found that the hardness decreases when going to the outer part of the oxide coating and also with [29, 30] which reported that anodic oxide layers with low thicknesses seem to be more effective in terms of friction. The behavior of the sample No 5 can be explained in a similar way but relatively low friction coefficient could be explained by the low value of surface roughness parameter *Ra*.

We are of the opinion that significant decrease in the friction coefficient behind the surface roughness and thickness depends also on dry lubrication film which is formed by the PEEK/BG material transfer. Moreover, a previous study indicated that admixture of IF-WS_2 [31] appear more effective in terms of friction.

In Figure 10, the surfaces of sample 4 before (Figure 10a) and after (Figure 10b) the tribological test and

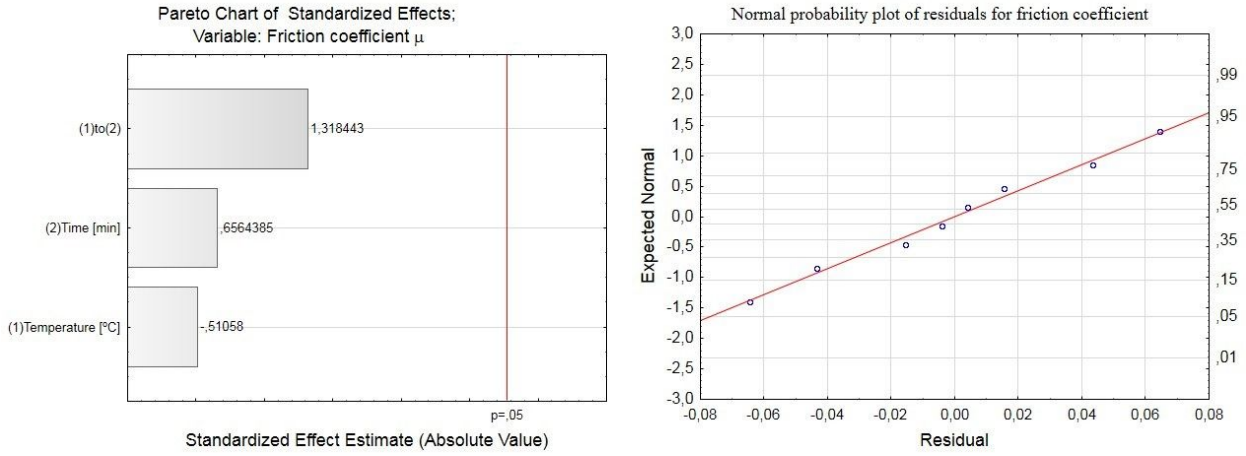

Figure 9: a) The Pareto chart of standardized effects for friction coefficient μ, b) the graphs of the normal probability plot of residual for friction coefficient μ variable

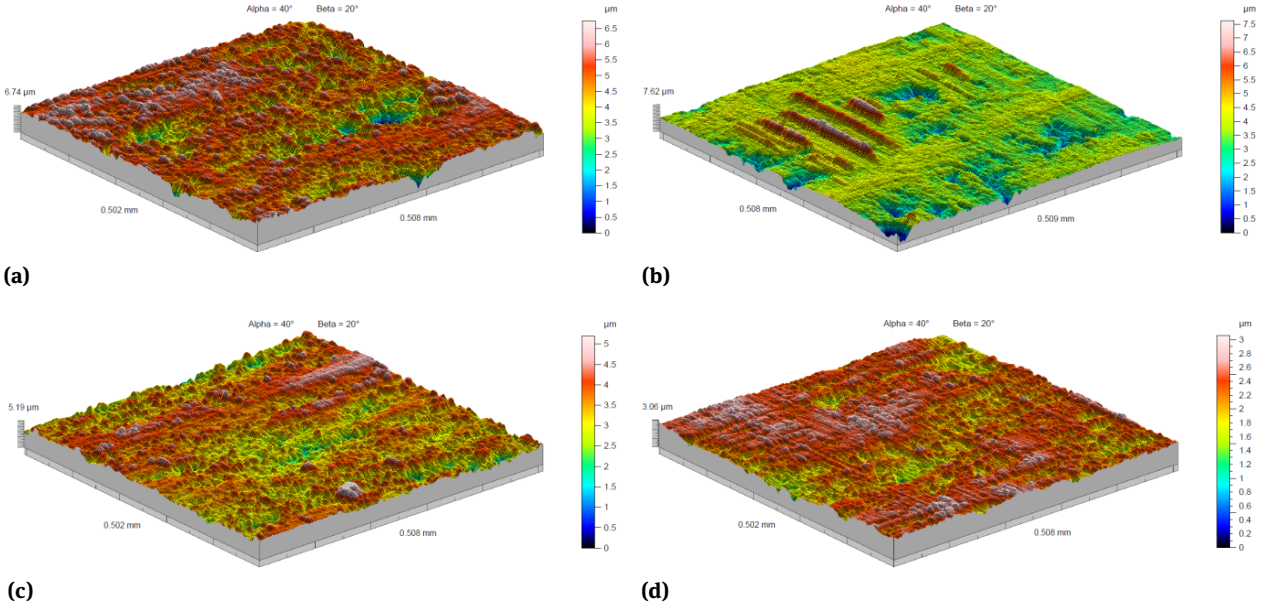

Figure 10: Isometric image a) of sample 4 before the tribological test b) of sample 4 after the tribological test c) of sample 5 before the tribological test d) of sample 5 after the tribological test

the surface of sample 5 before (Figure 10c) and after (Figure 10d) the tribological test are presented, respectively.

As it was mentioned above, the mass loss of PEEK/BG plastic during tribological friction with sample 4 was dependent on the surface roughness and also running-in time in sliding association. Moreover, Figure 10a shows that not only the Ra parameter but also the broadly understood surface texture affects the type of tribological behavior. For the sample 5, where the lowest value of friction coefficient and low mass loss of PEEK/BG plastic were observed, the surface texture (Figure 10c) allows for creating dense and more homogeneous sliding film of PEEK/BG resulting lower value of friction coefficient and mass loss of PEEK/BG plastic.

4 Conclusion

This paper gives an account of the 2^k factorial design and multiple regressions which were used to determine the influence of electrolysis time and temperature on the tribological properties of coatings.

The results of DOE suggest:

- high positive correlation between oxide thickness and time of the anodizing process, which means that those technological parameter affected Al_2O_3/IF-WS_2 oxide thickness;
- moderate positive correlation and negligible correlation between *Ra* surface roughness parameters before and after the tribological test respectively and time and temperature of the anodizing process, which implies that apart from the *Ra* parameter, there are other surface features that determine the nature of tribological cooperation, for example texture of Al_2O_3/IF-WS_2 oxide coatings;
- low positive correlation between friction coefficient and time and temperature of the anodizing process, this result seems to suggest that the analyzed technological parameters have no significant influence on the friction coefficient between the Al_2O_3/IF-WS_2 surface layers and PEEK/BG pin.

Despite this fact the present procedure of DOE could be for example applied to examine the influence of roughness surface and texture on friction coefficient between the sliding couple.

The findings of this study support the idea that the oxide layers with low thicknesses and low surface roughness parameter *Ra* seem to be more effective in terms of friction. Our research has highlighted that the stabilization of the friction coefficient indicates generation of stable anti-wear and anti-seizure Al_2O_3/IF-WS_2 oxide coatings.

The methodology presented in this paper may be also useful for similar investigations in automotive investigations [32] or quality management system [33]. The obtained results are also an inspiration for a wider use of image analysis methods [34, 35], even enhanced by a bootstrap-based analysis [36], that will allow for a more detailed description of the obtained surface. The application of the DOE methods presented in this article can be very interesting in similar approaches, such as pre-processing the output variable [37], searching for optimal settings [38, 39] or optimizing process performance while limiting its variability – using the Taguchi [40] or Shainin [41] methods.

References

[1] Kwolek P. Hard anodic coatings on aluminum alloys. Adv Manuf Sci Technol. 2017;41(3):35–46.
[2] Ardelean M, Lascău S, Ardelean E, Josan A. Surface treatments for aluminium alloys. IOP Conf Ser Mater Sci Eng. 2018;294(1).
[3] Remešová M, Tkachenko S, Kvarda D, Ročňáková I, Gollas B, Menelaou M, et al. Effects of anodizing conditions and the addition of Al2O3/PTFE particles on the microstructure and the mechanical properties of porous anodic coatings on the AA1050 aluminium alloy. Appl Surf Sci. 2020;513(August 2019).
[4] Mahmoud ERI, Algahtani A, Khan SZ, Ahmed GMS. Characterizations of Cladded 6082-T6 Aluminum Alloy Through Hard Anodizing. Sci Adv Mater. 2020;
[5] Rivero PJ, Maeztu JD, Berlanga C, Miguel A, Palacio JF, Rodriguez R. Hydrophobic and Corrosion Behavior of Sol-Gel Hybrid Coatings Based on the Combination of TiO2 NPs and Fluorinated Chains for Aluminum Alloys Protection. Metals (Basel). 2018;8(12).
[6] Du YJ, Damron M, Tang G, Zheng H, Chu CJ, Osborne JH. Inorganic/organic hybrid coatings for aircraft aluminum alloy substrates. Prog Org Coatings. 2001;41(4):226–32.
[7] Kmita T, Bara M. Surface oxide layers with an increased carbon content for applications in oil-Less tribological systems. Chem Process Eng – Inz Chem i Proces. 2012;
[8] Bara M, Skoneczny W, Kaptacz S. Tribological properties of ceramic-carbon surface layers obtained in electrolytes with a different graphite content. Eksploat i Niezawodn. 2008;
[9] Posmyk A. Influence of aluminium oxidation on insulation properties of oxide coating. Surf Eng [Internet]. 2019;35(7):573–7. Available from: https://doi.org/10.1080/02670844.2018.1542054
[10] Tomassi P, Buczko Z, Olkowicz K. The influence of anodic oxidation parameters on the growth rate of oxide coatings on aluminium. Inżynieria Powierzchni. 2018;
[11] Tsyntsaru N, Kavas B, Sort J, Urgen M, Celis JP. Mechanical and frictional behaviour of nano-porous anodized aluminium. Mater Chem Phys [Internet]. 2014;148(3):887–95. Available from: http://dx.doi.org/10.1016/j.matchemphys.2014.08.066
[12] Renaud A, Bonnaud L, Dumas L, Zhang T, Paint Y, Fasano F, et al. A benzoxazine/substituted borazine composite coating: A new resin for improving the corrosion resistance of the pristine benzoxazine coating applied on aluminum. Eur Polym J [Internet]. 2018;109(October):460–72. Available from: https://doi.org/10.1016/j.eurpolymj.2018.10.018
[13] Zhong X, Wu X, Jia Y, Liu Y. Self-repairing vanadium-zirconium composite conversion coating for aluminum alloys. Appl Surf Sci [Internet]. 2013;280:489–93. Available from: http://dx.doi.org/10.1016/j.apsusc.2013.05.015
[14] Jozwik J, Dziedzic K, Paszeczko M, Barszcz M. Comparative assessment of tribological properties of selected polymers and polymer composites. In: 2019 IEEE International Workshop on Metrology for AeroSpace, MetroAeroSpace 2019 – Proceedings. 2019.
[15] Laux KA, Jean-Fulcrand A, Sue HJ, Bremner T, Wong JSS. The influence of surface properties on sliding contact temperature and friction for polyetheretherketone (PEEK). Polymer (Guildf). 2016;
[16] Onodera T, Nunoshige J, Kawasaki K, Adachi K, Kurihara K, Kubo M. Structure and Function of Transfer Film Formed from PTFE/PEEK Polymer Blend. J Phys Chem C. 2017.

[17] Korzekwa J, Skoneczny W, Dercz G, Bara M. Wear mechanism of Al2O3/WS2 with PEEK/BG plastic. J Tribol. 2014;
[18] Wagner JR, Mount EM, Giles HF. Extrusion: The Definitive Processing Guide and Handbook: Second Edition. Extrusion: The Definitive Processing Guide and Handbook: Second Edition. 2013.
[19] Montgomery DC. Introduction to Statistical Quality Control, Sixth Edition. John Wiley & Sons, Inc. 2009.
[20] Pierlot C, Pawlowski L, Bigan M, Chagnon P. Design of experiments in thermal spraying: A review. Surf Coatings Technol. 2008;
[21] Pietraszek J, Radek N, Konrad B. Advanced statistical refinement of surface layer's discretization in the case of electro-spark deposited carbide-ceramic coatings modified by a laser beam. Solid State Phenom. 2013;197:198–202.
[22] Ruiz-Luna H, Lozano-Mandujano D, Alvarado-Orozco JM, Valarezo A, Poblano-Salas CA, Trápaga-Martínez LG, et al. Effect of HVOF processing parameters on the properties of NiCoCrAlY coatings by design of experiments. J Therm Spray Technol. 2014;23(6):950–61.
[23] Witz K, Hinkle DE, Wiersma W, Jurs SG. Applied Statistics for the Behavioral Sciences. J Educ Stat. 1990;
[24] Montero-Moreno JM, Sarret M, Müller C. Influence of the aluminum surface on the final results of a two-step anodizing. Surf Coatings Technol. 2007;201(14):6352–7.
[25] Aerts T, Dimogerontakis T, De Graeve I, Fransaer J, Terryn H. Influence of the anodizing temperature on the porosity and the mechanical properties of the porous anodic oxide film. Surf Coatings Technol. 2007;201(16–17):7310–7.
[26] Henley VF. The Surface Treatment and Finishing of Aluminium and its Alloys. Br Corros J. 1974;
[27] Lubas J. Assessment and application of TiB2 coating in sliding pair under lubrication conditions. Wear. 2012;
[28] Yerokhin AL, Nie X, Leyland A, Matthews A, Dowey SJ. Plasma electrolysis for surface engineering. Surf Coatings Technol. 1999;122(2–3):73–93.
[29] Guezmil M, Bensalah W, Khalladi A, Elleuch K, De-Petris Wery M, Ayedi HF. Effect of Test Parameters on the Friction Behaviour of Anodized Aluminium Alloy. Int Sch Res Not. 2014;2014:1–9.
[30] Fratila-Apachitei LE, Duszczyk J, Katgerman L. AlSi(Cu) anodic oxide layers formed in H2SO4 at low temperature using different current waveforms. Surf Coatings Technol. 2003;165(3):232–40.
[31] Korzekwa J, Bara M, Pietraszek J, Pawlus P. Tribological behaviour of Al2O3/inorganic fullerene-like WS2 composite layer sliding against plastic. Int J Surf Sci Eng. 2016;
[32] Pacana A, Czerwińska K, Bednárová L. Discrepancies analysis of casts of diesel engine piston. Metalurgija. 2018;
[33] Malindžák D, Pacana A, Pačaiova H. An effective model for the quality of logistics and improvement of environmental protection in a cement plant. Przem Chem. 2017;
[34] Gadek-Moszczak A. History of stereology. Image Anal Stereol. 2017;36(3):151–2.
[35] Wojnar L, Gadek-Moszczak A, Pietraszek J. On the role of histomorphometric (stereological) microstructure parameters inthe prediction of vertebrae compression strength. Image Anal Stereol. 2019;38(1):63–73.
[36] Gądek-Moszczak, A., Pietraszek, J., Jasiewicz, B., Sikorska, S., Wojnar L. The Bootstrap Approach to the Comparison of Two Methods Applied to the Evaluation of the Growth Index in the Analysis of the Digital X-ray Image of a Bone Regenerate. Stud Comput Intell [Internet]. 2015;572(January):127–36. Available from: http://www.scopus.com/inward/record.url?eid=2-s2.0-84921478623&partnerID=tZOtx3y1
[37] Pietraszek J, Goroshko A. The heuristic approach to the selection of experimental design, model and valid pre-processing transformation of DoE outcome. In: Advanced Materials Research. 2014.
[38] Skrzypczak-Pietraszek E, Reiss K, Żmudzki P, Pietraszek J. Enhanced accumulation of harpagide and 8-O-acetyl-harpagide in Melittis melissophyllum L. agitated shoot cultures analyzed by UPLC-MS/ MS. Vol. 13, PLoS ONE. 2018. 1–34 p.
[39] Dwornicka R, Radek N, Krawczyk M, Osocha P, Pobędza J. The laser textured surfaces of the silicon carbide analyzed with the bootstrapped tribology model. In: METAL 2017 – 26th International Conference on Metallurgy and Materials, Conference Proceedings. 2017.
[40] Pacana A, Gazda A, Malindzak D. Study on improving the quality of stretch film by Taguchi method. Przem Chem. 2013;92(6):980–2.
[41] Pacana A, Gazda A, Malindzak D, Stefko R. Study on improving the quality of stretch film by Shainin method. Przem Chem. 2014.